

Dark soliton decay due to trap anharmonicity in atomic Bose-Einstein condensates

N.G. Parker^{1,2}, N. P. Proukakis^{1,3} and C. S. Adams¹

¹ *Department of Physics, Durham University, Durham, DH1 3LE, United Kingdom*

² *School of Food Science and Nutrition, University of Leeds, Leeds, LS2 9JT, United Kingdom*

³ *School of Mathematics and Statistics, University of Newcastle, Newcastle upon Tyne, NE1 7RU, United Kingdom*

A number of recent experiments with nearly pure atomic Bose-Einstein condensates have confirmed the predicted dark soliton oscillations when under harmonic trapping. However, a dark soliton propagating in an inhomogeneous condensate has also been predicted to be unstable to the emission of sound waves. Although harmonic trapping supports an equilibrium between the co-existing soliton and sound, we show that the ensuing dynamics are sensitive to trap anharmonicities. Such anharmonicities can break the soliton-sound equilibrium and lead to the net decay of the soliton on a considerably shorter timescale than other dissipation mechanisms. Thus, we propose how small realistic modifications to existing experimental set-ups could enable the experimental observation of this decay channel.

PACS numbers: 03.75.Lm, 03.75.Hh, 05.45.Yv

I. INTRODUCTION

Dark solitons are one-dimensional phase defects that play an important role in nonlinear transport. They have been observed experimentally in nonlinear optics [1], shallow liquids [2], magnetic films [3] and, most recently, ultra-cold atomic Bose-Einstein Condensates (BECs) [4, 5, 6, 7, 8, 9, 10, 11]. In the latter case matter-wave dark solitons consist of a localised dip in the atomic density and a phase slip, and are supported by repulsive atomic interactions. Dark solitons are prone to several dissipation mechanisms. Two such mechanisms are thermal dissipation [12, 13, 14, 15] and the snake instability whereby the soliton decays into vortex rings [16, 17, 18, 19, 20, 21]. Although numerous initial experiments showed such instabilities to severely limit the soliton lifetime [4, 5, 6, 7], they can nonetheless be heavily suppressed at ultracold temperatures and in highly-elongated trap geometries. Indeed, such techniques have led to the recent generation of long-lived dark solitons that made many complete oscillations in the trapped condensate [8, 9]. Matter wave dark solitons are also subject to an instability to acceleration through an inhomogeneous system [23, 24, 25, 26, 28]. We will demonstrate that this instability is a generic occurrence for dark solitons in trapped atomic BECs. Furthermore, we will show that, under appropriately engineered conditions, this can become the dominant decay mechanism and is within reach of being detected by current experiments.

Condensate dynamics at zero temperature obey a nonlinear wave equation known as the Gross-Pitaevskii equation [11]. In one-dimension and under a homogeneous potential, a dark soliton is an exact and integrable solution of this equation. The presence of an inhomogeneous potential (which is relevant in practically all BEC experiments) simultaneously accelerates the soliton and breaks this integrability, rendering it unstable and leading to the emission of sound waves [24]. Providing the potential is slowly varying the decay of the soliton energy E_s follows

a simple acceleration-squared law [25, 27, 29, 30],

$$\frac{dE_s}{dt} = -\kappa \left(\frac{d^2 x_s}{dt^2} \right)^2, \quad (1)$$

where x_s is the soliton position and κ is a coefficient that typically depends weakly on the local density and soliton speed. An analogous instability arises for dark solitons in nonlinear optics, induced by modifications in the optical nonlinearity, and led to the original derivation of the above power law [27, 29].

Importantly, for the common case of harmonic trapping, dark solitons have been predicted to undergo conservative dynamics in the zero temperature and one-dimensional limit [23, 24, 31, 32], oscillating back and forth in the trap. This appears to oppose the prediction of instability under acceleration. This anomaly can be reconciled by the fact that in a harmonic trap continuous reabsorption of the emitted sound stabilises the soliton against decay [25]. The importance of soliton-sound interactions was reinforced in [34], where it was shown that energy could be pumped into a dark soliton by driving a sound field in the condensate. It is interesting to note that a similar instability arises for a vortex accelerating in a trapped BEC and that they too appear to be stabilised within harmonic traps [33].

Harmonic traps appear to be a special case. Previous results indicate that deviations from harmonic trapping tend to induce dissipation of the soliton. Such instability has been observed, for example, for a dark soliton in modified harmonic traps [23, 25], interacting with localised barriers [20, 30, 31, 35, 36, 37], and moving through an optical lattice [38, 39] and disordered potential [40]. Motivated by this effect we study the soliton dynamics under several pertinent forms of confining potential. Crucially, we demonstrate that the presence of anharmonicities can destroy the soliton-sound equilibrium and lead to net decay of the soliton. This decay can be rapid and within current experimental soliton lifetimes, provided the gas is kept at a relatively low temperature. Importantly, this

paper demonstrates that the experimental observation of this decay mechanism is within reach of current long-lived soliton experiments [8, 9, 10].

We begin in Section II by outlining the theoretical framework and reviewing key properties of dark solitons and their dynamics in harmonic traps. Section III identifies various experimentally-relevant geometries for observing/inducing the emission of sound waves, firstly by introducing a finite cut-off to the harmonic trap, and then by focusing on soliton dynamics under anharmonic (gaussian; quartic) traps. In Section IV we relate our findings to the recent long-lived soliton experiments [8, 9] and suggest routes to detect this decay mechanism with only minor changes in their respective experimental set-ups. Our main conclusions are then summarised in Sec. V.

II. BACKGROUND & MODELING

A. Gross-Pitaevskii equation

At ultra-cold temperature and under weak atomic s -wave interactions the vast majority of the atoms in an atomic BEC reside in the same quantum state. The atomic BEC can then be parameterised by a macroscopic ‘wavefunction’ $\psi(\mathbf{r}, t)$. This can be expressed as $\psi(\mathbf{r}, t) = \sqrt{n(\mathbf{r}, t)} \exp[i\theta(\mathbf{r}, t)]$, where $n(\mathbf{r}, t)$ is the atomic density distribution and $\theta(\mathbf{r}, t)$ is the condensate phase which can, in turn, be related to a fluid velocity via $v(\mathbf{r}, t) = (\hbar/m)\nabla\theta(\mathbf{r}, t)$. This wavefunction is described by the Gross-Pitaevskii equation (GPE) [41],

$$i\hbar \frac{\partial \psi(\mathbf{r}, t)}{\partial t} = \left(-\frac{\hbar^2}{2m} \nabla^2 + V_{\text{ext}}(\mathbf{r}) + g|\psi(\mathbf{r}, t)|^2 \right) \psi(\mathbf{r}, t). \quad (2)$$

Here m is the atomic mass and $g = 4\pi\hbar^2 a_s/m$ characterises the nonlinear atomic interactions, where a_s is the s -wave scattering length. The chemical potential of the condensate is denoted by μ . The external confining potential $V_{\text{ext}}(\mathbf{r})$ is typically harmonic with the form,

$$V_{\text{ext}}(\mathbf{r}) = \frac{1}{2}m [\omega_r^2 (x^2 + y^2) + \omega_z^2 z^2], \quad (3)$$

where we have assumed cylindrical symmetry, and where ω_r and ω_z are the harmonic trap frequencies in the radial and axial directions, respectively. Assuming a highly-elongated condensate ($\omega_z \ll \omega_r$) with tight radial confinement ($\hbar\omega_r > \mu$), the condensate dynamics become quasi-one-dimensional and the 1D version of the GPE [13, 16, 24, 25] becomes applicable. (This also assumes that fluctuations in the condensate phase can be ignored, which is justified at such low temperatures [42].)

We will simulate the condensate dynamics using the 1D GPE. This is performed by numerically propagating the wavefunction $\psi(z, t)$ on a discrete spatial grid using the Crank-Nicholson technique [46]. Although the energy of the soliton technically extends to infinity, we can

numerically evaluate a meaningful local estimate as outlined in Appendix A. We present our results in terms of harmonic oscillator units where time, length and energy are measured in units of ω_z^{-1} , $l_z = \sqrt{\hbar/m\omega_z}$ and $\hbar\omega_z$, respectively. The profile of the background condensate on which the soliton is imposed is specified by the ratio $(\mu/\hbar\omega_z)$. For $\mu \gg \hbar\omega_z$, the system is in the Thomas-Fermi regime. Here the density profile can be approximated by $n(\mathbf{r}) = [\mu - V(\mathbf{r})]/g$ and the system is much wider than the soliton. In the opposite limit of $\mu \ll \hbar\omega_z$ the system is closer to the non-interacting limit with size comparable to the soliton size. Throughout this work and unless otherwise stated we will employ a system defined by $\mu = 22.4\hbar\omega_z$, which is well within the Thomas-Fermi regime.

B. Properties of dark solitons

In 1D and on a uniform background density n_0 a dark soliton with speed v and position $(z - vt)$ has the analytical form,

$$\psi(z, t) = \sqrt{n_0} e^{-i(\mu/\hbar)t} \left(\beta \tanh \left[\beta \frac{(z - vt)}{\xi} \right] + i \left(\frac{v}{c} \right) \right), \quad (4)$$

where $\beta = \sqrt{1 - (v/c)^2}$ and the healing length $\xi = \hbar/\sqrt{mn_0g}$ characterises the soliton width. For this homogeneous case the chemical potential is given by $\mu = n_0g$. The soliton speed v is related to both the soliton depth n_d (with respect to the background density) and the total phase slip S across the centre via $v = \sqrt{n_0 - n_d} = c \cos(S/2)$, where $c = \sqrt{n_0g/m}$ is the Bogoliubov speed of sound. A stationary soliton has a π phase slip and a maximum depth $n_d = n_0$, while a soliton with speed c is indistinguishable from the background fluid.

The energy of the dark soliton of Eq. (4), which is an ideal quantity for parameterising the soliton behavior, is given by,

$$E_s = \frac{4}{3}\hbar n_0 c \left[1 - \left(\frac{v}{c} \right)^2 \right]^{3/2}. \quad (5)$$

Accordingly, the dissipation of energy from the soliton is associated with an *increase* in its speed. Under an inhomogeneous potential the soliton behaves, to first order, as an effective particle of negative mass [45]. The soliton will tend to oscillate when confined within a trap and any dissipation is associated with an increase in the amplitude of the soliton oscillations, an effect termed “anti-damping” [23]. For the specific case of a harmonic trap a dark soliton is predicted to oscillate at a frequency $\omega_s = \omega_z/\sqrt{2}$ [12, 16, 23, 24, 25, 26, 31, 32]. Note that deviations from this prediction can arise due to the dimensionality of the system [43], the presence of other solitons and trap anharmonicities, and these effects have been recently observed experimentally [8, 9].

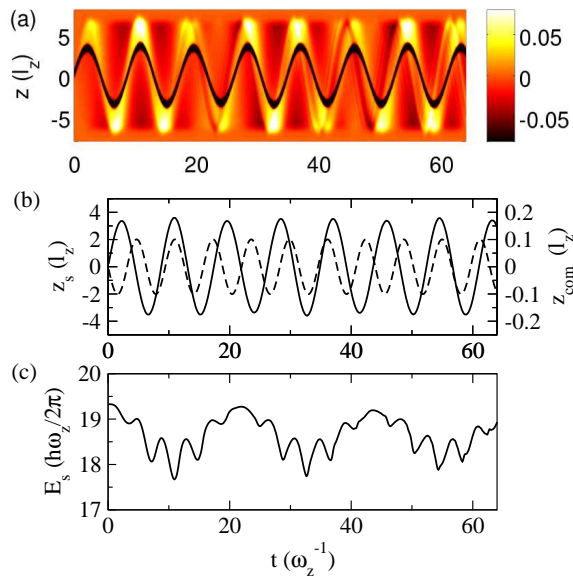


FIG. 1: (Color online) Dark soliton dynamics in a harmonically-trapped condensate for a soliton initially located at the trap centre and with a speed $v_0 = 0.5c$. (a) Renormalised density $|\psi(z,t)|^2 - n_{\text{TI}}(z)$, in units of the peak density n_0 . (b) Soliton position $z_s(t)$ (solid line, left axis) and condensate centre of mass $z_{\text{com}}(t)$ (dashed line, right axis). The soliton position z_s is defined as the point of the soliton density minimum. (c) Soliton energy $E_s(t)$, determined numerically as outlined in Appendix A.

C. Dark solitons in purely harmonic traps

We first review the dynamics of a dark soliton in a 1D harmonic trap $V(z) = m\omega_z^2 z^2/2$, which has been the subject of much theoretical work [12, 16, 23, 24, 25, 31, 32]. The initial state is $\psi(z,0) = \sqrt{n_{\text{TI}}(z)}\psi_s(z,0)$, where $n_{\text{TI}}(z)$ is the time-independent background density obtained by imaginary time propagation of the GPE [44] and the soliton solution $\psi_s(z,0)$ is given by Eq. (4). The dark soliton solution is centred at the origin, where the density is locally homogeneous, and has initial speed v_0 .

The typical evolution of a dark soliton in a harmonically-confined BEC is shown in Fig. 1(a). The soliton (dark density dip) oscillates sinusoidally through the BEC. This is accompanied by small-scale density excitations of the background condensate, of amplitude $\sim 0.1n_0$. We attribute these to the sound waves emitted from the accelerating soliton. The sound waves remain confined within the system and form a dipole (sloshing) mode of the condensate. We have tracked the soliton trajectory z_s (solid line in Fig. 1(b)) and taken its Fourier spectrum (solid line in Fig. 2(a)). This confirms that the soliton primarily oscillates at frequency $\omega_s \approx \omega_z/\sqrt{2}$, in agreement with previous predictions [12, 16, 23, 24, 31]. The spectrum features a secondary frequency component at $\omega = \omega_z$, which arises due to the interaction of the soli-

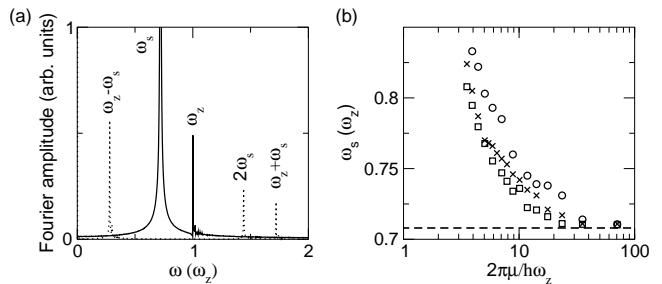


FIG. 2: (a) Fourier spectrum of $z_s(t)$ (solid line) and $E_s(t)$ (dotted line) for the case in Fig. 1. (b) Average soliton frequency ω_s as a function of the system parameter $(\hbar\omega_z/\mu)$ for $v_0 = 0.25c$ (squares), $v_0 = 0.5c$ (crosses) and $v_0 = 0.75c$ (circles). The analytic prediction, $\omega_s^0 = \omega_z/\sqrt{2}$, is shown (dashed line).

ton with the dipole mode of the condensate.

During these dynamics the condensate centre-of-mass oscillates due to the linear momentum introduced by the imposed soliton solution. The condensate centre-of-mass $z_{\text{com}} = \int_{-\infty}^{+\infty} z|\psi(z)|^2 dz/N$ is plotted in Fig. 1(b) (dashed line, right axis). The centre-of-mass motion is decoupled from the “internal” dynamics of the condensate and oscillates sinusoidally at the trap frequency ω_z , as noted in [23]. The soliton energy E_s (solid line in Fig. 1(c)), whose definition is outlined in Appendix A, remains constant on average, but features oscillations. The corresponding Fourier spectrum (dotted line in Fig. 2(a)) has contributions from $2\omega_s$ and beat frequencies between the soliton and dipole mode, e.g. $(\omega_z - \omega_s)$, $(\omega_z + \omega_s)$, plus higher order combinations (not visible in Fig. 2).

The system considered here is in the Thomas-Fermi regime $\mu \gg \hbar\omega_z$ (with $\mu = 22.4\hbar\omega_z$). We have also analysed the soliton motion over a range of values of $(\mu/\hbar\omega_z)$ with the results shown in Fig. 2(b). For $\mu \gg \hbar\omega_z$ the soliton oscillation frequency ω_s agrees with the analytic prediction of $\omega_s \approx \omega_z/\sqrt{2}$ [12, 16, 23, 31]. Indeed, these predictions are based on treating the soliton as a classical particle and so is valid when the soliton is small compared to the system size. As the system parameter $(\mu/\hbar\omega_z)$ is reduced (which reduces the size of the system relative to the soliton size), ω_s deviates from this prediction and becomes dependent on the soliton speed. For $\mu = 5\hbar\omega_z$, which is when the system size is comparable to the soliton size, ω_s can be over 10% larger than the analytic predictions. Note that in all cases considered, the soliton dynamics undergo no net decay. Furthermore, the frequency component at ω_z is present throughout the range of systems tested. Note that shifts in the soliton oscillation frequency can also arise due to the presence of the transverse direction [8, 43] and this is distinct to our present 1D analysis.

We attribute the density excitations in the system to sound waves emitted by the unstable accelerating soliton. Although these waves co-exist with the soliton at long times, it takes a finite time from $t = 0$ for the emitted

sound waves to reflect off the edge of the condensate and reinteract with the soliton. This will be approximately half a trap period $t \approx \pi\omega_z^{-1}$. Close inspection of Fig. 1(c) shows that the soliton energy decays monotonically at these early times. Indeed, for this time the decay follows the acceleration-squared law of Eq. (1). After this time the soliton energy is found to oscillate between its initial value and some lower value, providing a clear indication of the reabsorption of sound by the soliton.

A recent study by Pelinovsky *et al.* [26] has considered the motion of a dark matter-wave soliton in a harmonic trap by means of an asymptotic multiscale expansion method. Sound radiation in the system is predicted to oscillate at the same frequency as the soliton, thereby causing the periodic re-interaction of the sound and soliton, and thus enabling reabsorption by the soliton. This prediction is somewhat consistent with our observations, although we observe the sound waves to have oscillatory components at the trap frequency as well as the soliton frequency.

We now discuss various geometries in which the emitted sound waves can be studied.

III. PROBING ANHARMONICITY-INDUCED SOLITON DECAY

A. Dark soliton dynamics in a cut-off harmonic trap

Although a purely harmonic trap generates no net decay of the dark soliton, we can nonetheless probe the existence of sound emission even within harmonic traps by introducing a finite cut-off to the trap, as discussed in [25]. We thus consider a cut-off harmonic trap of the form,

$$V_{\text{ext}}(z) = \begin{cases} m\omega_z^2 z^2/2 & \text{for } |z| < \sqrt{2V_0/m\omega_z^2} \\ V_0 & \text{for } |z| > \sqrt{2V_0/m\omega_z^2} \end{cases} \quad (6)$$

where V_0 specifies the magnitude of the cut-off. Although this potential is somewhat unphysical, it can be approximated by employing a tight dimple trap embedded within a weaker ambient trap (i.e. an effective double-trap geometry) [25]. Since sound waves have an energy of approximately the chemical potential μ , the cut-off depth enables control between a regime where the sound waves remain confined to the inner trap ($V_0 \gg \mu$) and a regime where they can escape the inner trap ($V_0 < \mu$). In Fig. 3 we show the evolution of the system for various values of V_0 which illustrate these regimes. For $V_0 = 1.2\mu$ (Fig. 3(a)) the sound waves are confined to the harmonic region and the evolution is essentially identical to that under pure harmonic trapping (Fig. 1(a)). For this case the soliton energy, presented in Fig. 4(a), shows no net decay. For $V_0 = 0.8\mu$ (Fig. 3(c)) all of the emitted sound waves escape the harmonic region and propagate outwards. The soliton energy (Fig. 4(a)) decays monotonically and follows the acceleration-squared law of Eq. (1) [25]. Note

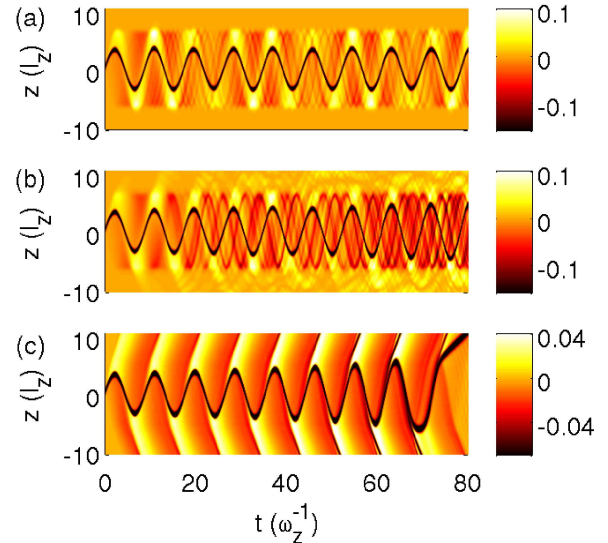


FIG. 3: (Color online) Space-time plots of renormalised density ($|\psi(z, t)|^2 - n_{\text{TI}}(z)$) showing the dynamics of a $v_0 = 0.5c$ dark soliton in cut-off harmonic trap with (a) $V_0/\mu = 1.2$, (b) 1.05 and (c) 0.8. The dark soliton appears as a black line, while sound waves appear as light/dark areas.

that at late times the soliton has anti-damped sufficiently that it escapes to the outer homogeneous region where it propagates with constant speed. In between these regimes, e.g. for $V_0 = 1.05\mu$ (Fig. 3(b)), only a fraction of the sound waves escape to infinity, and we observe a slower decay of the soliton. Note that the power law of Eq. (1) no longer applies since considerable sound reabsorption occurs. The emitted sound remains mostly confined to the central trap and the amplification of this sound field as the soliton decays is clearly evident.

For the cut-off harmonic trap, decay of the soliton occurs because sound waves escape the harmonic region and carry away their energy. For $V_0 < \mu$ this can always happen. However, it is important to understand how decay changes as V_0 becomes greater than μ , as this will prove crucial in our subsequent discussion on soliton decay in experimentally relevant gaussian traps. We define a decay time t_d as the time for the soliton to become indistinguishable from the background condensate. In Fig. 4(b) we show how the decay rate t_d^{-1} varies as V_0 becomes greater than μ . The most important thing to note is that the decay rate drops very quickly with V_0 . For the soliton speed $v_0 = 0.5c$, which we have considered in Fig. 3, decay ceases for $V_0 \geq 1.15\mu$. This corresponds to the point at which sound waves no longer escape the harmonic region. This threshold is larger for faster solitons. For example, for $v_0 = 0.75c$, decay is ultimately prevented for $V_0 \geq 1.4\mu$. This suggests that the sound waves emitted by faster solitons are of higher energy. However there always exists a threshold cut-off depth beyond which the tendency to decay is suppressed.

Having reviewed and extended previous results of dark

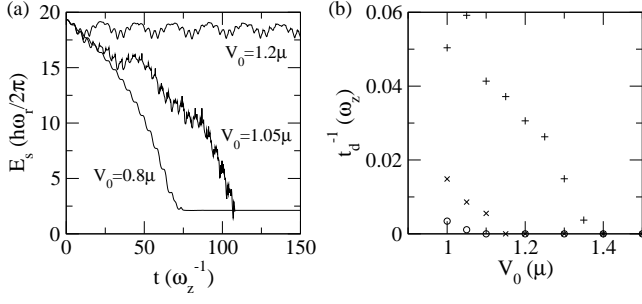


FIG. 4: (a) Evolution of the soliton energy E_s in a cut-off harmonic trap for $V_0/\mu = 0.8, 1.05$ and 1.2 for initial speed $v_0 = 0.5c$. (b) Decay rate t_d^{-1} as a function of trap cut-off V_0 for $v_0 = 0.25c$ (circles), $v_0 = 0.5c$ (crosses) and $v_0 = 0.75c$ (pluses).

soliton dynamics in harmonic traps we now progress to consider an important additional decay mechanism for dark solitons, namely their propagation in condensates under anharmonic confinement.

B. Dark soliton dynamics in a gaussian trap

For simplicity, and in order to make contact with realistic experiments, we begin by considering a gaussian trap; such traps are commonly used experimentally and are formed in the cross-section of an off-resonant laser beam. Notably, the recent dark soliton experiment of Becker *et al.* [9] was performed in a trap which was gaussian in the longitudinal direction. We will focus on this particular experiment further in Section V. However, in this section we will present the general dynamics in a gaussian trap.

We consider here a 1D gaussian trap of the form,

$$V_{\text{ext}}(z) = V_0 \left[1 - \exp\left(\frac{-m\omega_z^2 z^2}{2V_0}\right) \right] \quad (7)$$

$$= \frac{m}{2}\omega_z^2 z^2 - \frac{V_0}{2} \left(\frac{m\omega_z^2 z^2}{2V_0}\right)^2 + \frac{V_0}{3} \left(\frac{m\omega_z^2 z^2}{2V_0}\right)^3 + \dots$$

The leading term in the Taylor expansion is harmonic, with trap frequency ω_z , while the higher order terms are anharmonic. In a similar manner to the cut-off trap, the parameter V_0 controls whether sound waves can escape the system. However, we will generally consider the regime $V_0 > \mu$, where the condensate (including soliton and sound) is wholly confined to the gaussian trap. Importantly, the gaussian depth V_0 also controls the degree of anharmonicity experienced by the condensate, and can be varied experimentally by varying the laser intensity. In the limit $V_0 \gg \mu$, the confinement is effectively harmonic, while for $V_0 \sim \mu$ the condensate will experience strong anharmonic terms.

We first consider how the gaussian depth affects the soliton dynamics, with Fig. 5 showing the density evolution for three values of V_0 . For $V_0 = 5\mu$ [Fig. 5(a)], the

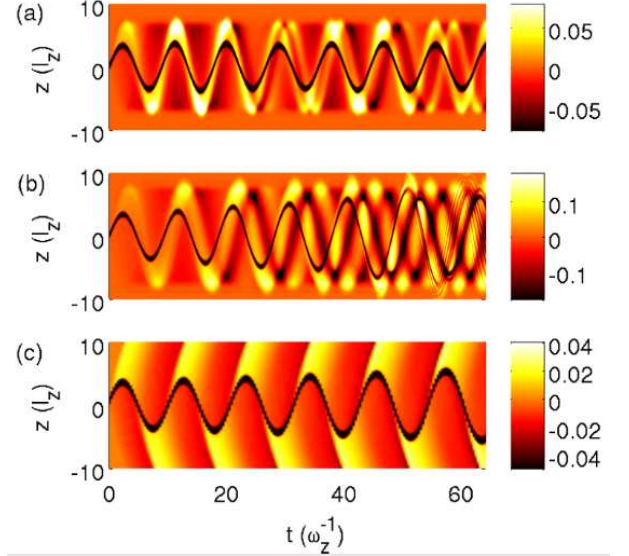


FIG. 5: Space-time plots of renormalised density $(|\psi(z, t)|^2 - n_{\text{TI}}(z))$ showing the dynamics of a $v_0 = 0.5c$ dark soliton in a (a) deep gaussian trap with $V_0 = 5\mu$, (b) shallow gaussian trap with $V_0 = 2\mu$, and (c) infinite system with $V_0 = 0.8\mu$.

trapping is effectively harmonic and the dynamics are similar to those in a harmonic trap, with the soliton energy, shown in Fig. 6(a), undergoing no net decay. As for the purely harmonic trap this occurs due to the complete reabsorption of the emitted sound by the soliton.

In contrast, for $V_0 = 2\mu$ (Fig. 5(b)), the soliton amplitude increases and its energy decreases (Fig. 6(a)). The soliton decay is accompanied by the growth of sound waves in the system. After only 5 oscillations ($t \approx 50\omega_z^{-1}$) the soliton is so fast and shallow that it is indistinguishable from the sound field. It is important to note here that the trap depth is sufficiently large that no sound waves escape the system and so the decay mechanism is quite distinct from that of the shallow cut-off harmonic trap. While the sound waves remain confined to the trap and co-exist with the soliton, they do not stabilise the decay. We believe that the anharmonic nature of the trap introduces a dephasing between the sound and soliton that prevents the sound from being completely reabsorbed. For completeness we also present the dynamics for $V_0 = 0.8\mu$ (Fig. 5(c)) where sound waves can escape the trap. In this case we observe the soliton undergoing decay with no sound reabsorption, similar to the corresponding case for the cut-off harmonic trap (Fig. 3(c)).

In Fig. 6(b) we plot the decay rate t_d^{-1} of the soliton versus the gaussian depth V_0 for various soliton speeds. Consider the case of $v_0 = 0.5c$ (crosses). Here decay occurs up to $V_0 = 3.5\mu$. Note that according to the results of Fig. 4(b) we expect that no sound can escape for $V_0 > 1.5\mu$ and so it is clear that the decay occurs even in the presence of the emitted sound. We see that the decay rate decreases with V_0 . This is consistent with the decay being due to anharmonicities: as V_0 increases the trap

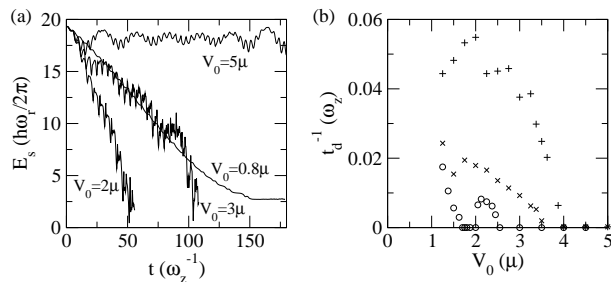


FIG. 6: (a) Evolution of the soliton energy E_s in a gaussian trap for various depths V_0 for a soliton with initial speed $v_0 = 0.5c$. (b) Decay rate t_d^{-1} as a function of V_0 for $v_0 = 0.25c$ (circles), $v_0 = 0.5c$ (crosses) and $v_0 = 0.75c$ (pluses).

becomes increasingly harmonic (from the perspective of the condensate). Furthermore we see that faster solitons have larger decay rates and undergo decay up to larger values of V_0 . We attribute this to the fact that faster solitons probe closer to the edge of the condensate where the trap anharmonicities have the largest effect.

It is important to note that the soliton decay in the gaussian trap can be considerable. For example, for the case presented in Fig. 5(b), the soliton has practically disappeared by $t = 50\omega_z^{-1}$, which corresponds to approximately 5 soliton oscillations in the trap. Assuming a typical trap frequency of $\omega_z = 2\pi \times 100$ Hz, this timescale corresponds to around 80 ms, which is well within the thermodynamic lifetime of dark solitons at ultralow temperatures [8, 9, 15]. Furthermore, the fastest decay presented in Fig. 6(b) occurs twice as fast as this example, corresponding to only two or three soliton oscillations.

C. Dark Soliton Dynamics in a Quartic Trap

To give further evidence of the role of trap anharmonicities in dark soliton decay we briefly consider the soliton dynamics within a quartic trap. Quartic potentials can be obtained, for instance, by modifying the gaussian potential from a laser beam, as performed experimentally to create harmonic-plus-quartic traps [47]. As such, we assume our quartic trap to have the form of the quartic term of the gaussian potential (Eq. 8), i.e.,

$$V_{\text{ext}}(z) = \frac{1}{2V_0} \left(\frac{m\omega_z^2 z^2}{2} \right)^2. \quad (8)$$

Following previous sections, we define our system via $\mu = 22.4\hbar\omega_z$, and assume here $V_0 = 10\mu$. In Fig. 7 we present the evolution of the soliton energy for various soliton speeds. We observe that the soliton stability is strongly dependent on speed. Slow solitons $v_0 \leq 0.5c$ undergo little or no detectable decay, while faster solitons, e.g. $v_0 = 0.8c$, do undergo decay. Note that the decay is significantly slower than in the gaussian trap.

We have also considered further traps formed by a combination of harmonic and quartic terms, and observe

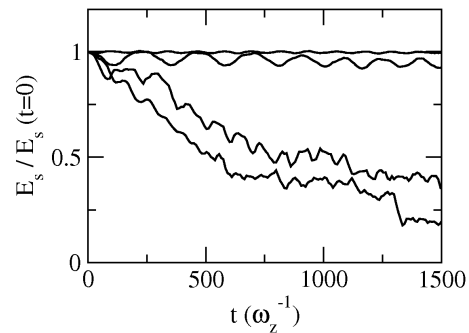


FIG. 7: (a) Evolution of the soliton energy E_s in a quartic trap for soliton speeds of (from top to bottom) $v_0/c = 0.5, 0.6, 0.7$ and 0.8 . The trap has the form of Eq. (8) with $V_0 = 10\mu$.

regimes of soliton decay in all cases. For a harmonic-plus-quartic trap, the trap has similar properties to the purely quartic trap and we obtain similar qualitative results. For a harmonic-minus-quartic trap, the trap is similar to a gaussian trap, particularly in the sense that it only has finite depth, and we find similar results to the gaussian trap.

We now discuss how our findings relate to recent experiments conducted at very low temperatures.

IV. APPLICATION TO RECENT EXPERIMENTS

In the early dark soliton experiments [4, 5, 6, 7] the solitons were short lived due to thermal dissipation and the snake instability. This limited the observation times to a fraction of the soliton oscillation period. Recent experiments [8, 9, 10] have heavily suppressed these dissipation mechanisms by operating at extremely cold temperatures and by employing quasi-1D geometries. As a result they were able to observe solitons over much longer timescales in which the soliton undergoes multiple oscillations in the trap. Indeed, in the experiment of Becker *et al.* [9] dark solitons were observed for over 2.8 s, corresponding to approximately 10 soliton oscillations in the trap. The considerable soliton lifetimes in these recent experiments, as well as the suppression of thermal dissipation and the snake instability, offer realistic opportunities to experimentally detect the acceleration-induced decay of the soliton discussed here.

A. Experiment of Becker et al.

We firstly consider the experiment of Becker *et al.* [9]. Dark solitons were generated in an elongated ^{87}Rb condensate via a phase imprinting technique and observed to oscillate in the trap with peak velocity $v_0 = 0.56c$. The trap, formed by the optical dipole force of an applied laser beam, featured a gaussian profile in the axial direction with waist $W_z = 125 \mu\text{m}$ and dominant harmonic

frequency $\omega_z = 2\pi \times 5.9$ Hz. For the experimentally-quoted peak density of $n_0 = 5.8 \times 10^{13} \text{ cm}^{-3}$ we estimate the chemical potential of the condensate to be $\mu/k_B \sim n_0 g/k_B \sim 23$ nk. The amplitude of the gaussian potential is $V_0 = m\omega_z^2 W_z^2/4 = 58$ nK. The important depth-to-chemical potential ratio is then $V_0/\mu \sim 2.5$. Based on these parameters our simulation gives a soliton oscillation frequency of $\omega_s = 2\pi \times 3.94$ Hz and an amplitude of $Z_0 \approx 34\mu\text{m}$, which are both in good agreement with the values quoted in Ref. [9].

It is pertinent to ask whether acceleration-induced decay of the soliton occurs in this system, and whether it may be detectable. In Fig. 8(a) we plot the soliton trajectory in the experimental system for several values of the trap depth V_0 . Note that the trap depth V_0 is proportional to, and can be varied by modifying, the intensity of the laser beam that forms the trap. For $V_0 = 4\mu$ (grey line) the trap is essentially harmonic: the soliton undergoes no discernable decay and oscillates with constant amplitude. For $V_0 = 2\mu$ (dotted line), which is just smaller than the number used in the experiments, the soliton experiences weak trap anharmonicities, causing it to decay slowly (as evident from the increase in the soliton amplitude) and effectively disappear by $t \sim 6$ s. This decay timescale is longer than the reported experimental lifetime (2.8 s), and so evidence of such decay would not be easily visible in the current experiment. Under a slight reduction in the trap depth to $V_0/\mu = 1.7$ (solid line) the soliton undergoes much quicker decay, disappearing into the background condensate after only 2.5 s. Importantly, this is now within the experimental soliton lifetime.

The effect of trap depth is shown in more detail in Fig. 8(b) which plots the decay time as a function of trap depth V_0 for two different initial soliton speeds. The maximum reported experimental soliton lifetime (2.8 s) is shown (dashed line) for reference. As earlier results indicated, the decay time generally increases with V_0 as the trap becomes increasingly harmonic. For the experimental trap depth $V_0 \sim 2.5\mu$ and soliton speed $v_0 = 0.56c$ the soliton decays over a timescale $t_d \approx 6$ s, which is longer than the experimental lifetime. How could one modify the experiment to make the decay occur within the experimental timescale? Firstly, this can be achieved (assuming an initial soliton speed of $v_0 = 0.56c$) by reducing the trap depth to the range $V_0 \lesssim 1.8\mu$. Secondly, the decay can be made more rapid by beginning with a faster soliton. For example, for $v_0 = 0.75c$ the soliton will decay within the experimental lifetime provided the trap depth does not exceed $V_0 \sim 2.8\mu$.

These results suggest that with only slight modifications this decay channel will dominate the experiment and cause the soliton to decay within the experimental timescale. The soliton dynamics are also very sensitive to the trap depth V_0 , a feature which also lends itself to experimental detection. The detectable signature for the decay would be provided by the considerable anti-damping of the soliton that accompanies the decay, which could be probed either in expansion images [4, 5, 8, 9, 10]

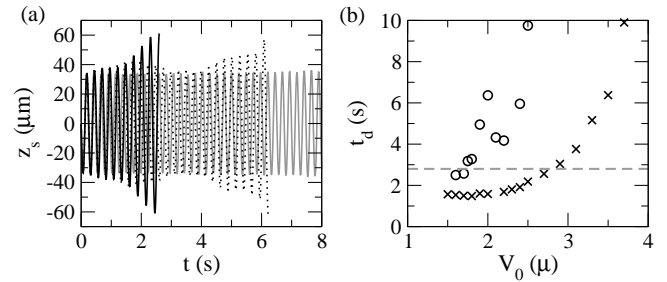


FIG. 8: Soliton decay in the experimental system of Ref. [9]. (a) The evolution of the soliton position for $V_0 = 1.7\mu$ (solid line), $V_0 = 2\mu$ (dotted line) and $V_0 = 4\mu$ (grey line). Following the experimental observations we employ an initial soliton speed of $v_0 = 0.56c$. (b) Decay time in the experimental system as a function of the gaussian trap depth V_0 . Initial soliton speeds of $v_0 = 0.56c$ (circles) and $v_0 = 0.75c$ (crosses) are presented. The dashed line indicates the maximum soliton lifetime reported in the experiment.

or even in situ [22].

B. Experiment of Weller et al.

We will also briefly discuss the recent soliton experiment by Weller *et al.* [8]. Two separated condensates were initially formed in a double trap potential. The double trap potential is formed by the combination of an elongated harmonic trap and one period of a one-dimensional optical lattice potential. Upon removal of the optical lattice the condensate underwent nonlinear interference which resulted in the production of dark solitons. These solitons were then observed to make up to 7 oscillations in the system. Although the solitons are typically produced in pairs we expect our predictions to hold for multiple solitons. The final trap potential is harmonic and so we do not expect any net decay of the solitons due to acceleration-induced sound emission. However, if the optical lattice potential were instead maintained at some low amplitude following the creation of the dark solitons, then we anticipate that soliton decay would occur.

We previously considered the dynamics of a dark soliton in a harmonic trap featuring an optical lattice potential [38]. The optical lattice potential was assumed to be weak (amplitude less than the chemical potential) such that the soliton could traverse the lattice site/s and thereby undergo acceleration-induced sound emission. Provided the lattice spacing λ was in the range $\xi < \lambda < 2L_z$, where ξ is the healing length and L_z is the condensate length, the soliton consistently underwent decay. (For $\lambda < \xi$ the density perturbations due to the optical lattice become smeared out while for $\lambda > 2L_z$ the trap reduces to being effectively harmonic.) This is consistent with the results presented in this paper: the optical lattice introduces anharmonicities that prevent complete sound reabsorption. The ensuing decay could be rapid, with complete decay occurring as quickly as

within one trap period in certain cases. In the experiment of Weller *et al.* [8] the lattice spacing is approximately L_z , and so we expect that the presence of the lattice can indeed induce soliton decay. This suggestion is similar to an earlier prediction [20] where we showed that a single gaussian barrier within a harmonic trap could lead to soliton decay. Moreover, decay in the experiment of [8] could be further enhanced by decreasing the periodicity of the proposed optical lattice; following previous results [38] we would expect the quickest decay when $\lambda \sim 5\xi$.

V. DISCUSSION

We have examined the zero-temperature, mean-field dynamics of dark solitons in atomic Bose-Einstein condensates under harmonic and anharmonic trapping. Such inhomogeneous potentials generally accelerate the soliton and induce an instability whereby the soliton radiates sound waves. In the absence of sound reabsorption the power radiated by the soliton is proportional to its acceleration squared. However, due to the finite-size of BECs, the sound waves remain in the system and generally re-interact with the soliton. The ensuing dynamics between the soliton and sound waves are crucially dependent on the form of the trapping potential.

Under harmonic trapping no net decay of the soliton is observed, despite the local instability of the soliton. The isochronicity of the harmonic trap leads to the creation of a dynamical equilibrium between the soliton and the emitted sound waves which prevents net soliton decay. We note that the inclusion of an additional harmonic frequency to the system, e.g., by considering an asymmetric harmonic trap (different trap frequencies for $z > 0$ and $z < 0$), maintains the stability of the soliton. Decay of the soliton in the harmonic trap can be induced, but involves removal of some of the emitted sound, e.g. by introducing a finite cut-off to the harmonic trap.

In a gaussian trap decay can occur without the removal of the emitted sound even at zero temperature. This is possible because the soliton-sound equilibrium is broken by the anharmonicity of the trap. In accord with this the decay is strongly dependent on the anharmonicity experienced by the soliton. The soliton decay is accompanied by the growth of short wavelengths in the sound field. Quartic trapping also leads to soliton decay. Furthermore, several existing studies have added some form of anharmonic perturbation to the harmonic trap and observed soliton decay, e.g. under the addition of an optical lattice [38, 39], a localised barrier [20, 31] and a disordered potential [40], in concurrence with our findings.

Soliton decay can be rapid. For example, in the gaussian trap we have observed a soliton (with initial speed $v_0 = 0.5c$, where c is the speed of sound) disappear into the sound field after only five oscillations in the trap. Given that solitons have recently been stabilised for over 7 trap oscillations [8, 9] it is clear that acceleration-induced soliton decay can dominate over the more well-

known dissipation mechanisms (thermal dissipation and the snake instability). For the experiment of Becker *et al.* [9], which was conducted in a gaussian trap, our results suggest that the soliton should completely decay within the experimental lifetime provided a slightly shallower gaussian trap or a faster soliton is employed. Note that the trap depth is readily varied through the intensity of the laser beam that forms the trap, while the soliton speed can be varied by adjusting the degree of phase imprinting. Furthermore, for the recent experiment of Weller *et al.* [8] we suggest that if a weak optical lattice is maintained during soliton propagation it may lead to significant soliton decay. Soliton decay can be detected by the increase in the soliton oscillation amplitude measured either in successive absorption images or in situ, with the accompanying growth of the sound field providing further indication of this effect.

It is interesting to note that the instability to acceleration that underpins this decay channel has also been predicted for vortical excitations in atomic BECs, including single vortices [33, 48, 49], corotating vortex pairs [50] and two-dimensional vortex-antivortex pairs [51]. Hybrid dark soliton/vortex rings excitations that have recently been observed [22, 52] may also be expected to undergo an instability to acceleration. As such the decay channel discussed here may extend well beyond dark solitons.

Acknowledgments

We acknowledge the UK EPSRC (NGP/NPP/CSA) and the Canadian Government (NGP) for support. We thank A. M. Martin, D. H. J. O'Dell, D. Pelinovsky and K. Sengstock for discussions.

APPENDIX A: EVALUATION OF THE DARK SOLITON ENERGY

Although the soliton energy technically extends up to the boundary of the system it is useful to have a *local* measurement of the soliton energy. We perform this by numerically evaluating the energy in a local region about the soliton centre. In trapped systems this will typically contain contributions from other excitations, e.g. sound waves. However, this contribution is typically very small. Note that from an experimental point of view it is precisely the behaviour of this soliton region, including local excitations, which is probed experimentally.

The energy density of the condensate is given by the energy functional,

$$\varepsilon[\psi] = \frac{\hbar^2}{2m} |\nabla\psi|^2 + V_{\text{ext}} |\psi|^2 + \frac{g}{2} |\psi|^4. \quad (\text{A1})$$

We define our soliton energy E_s to be,

$$E_s = \int_{z_s - z_{\text{int}}}^{z_s + z_{\text{int}}} \varepsilon[\psi] dz - \int_{z_s - z_{\text{int}}}^{z_s + z_{\text{int}}} \varepsilon[\sqrt{n_{\text{TI}}}] dz. \quad (\text{A2})$$

Here z_{int} defines the extent of the integration region. Note that we subtract off the corresponding energy of the condensate background density (second term). Figures 9(a) and (b) present the integrated soliton energy as a function of z_{int} for various soliton speeds and background densities, respectively. For simplicity we consider an infinite system with $V(z) = 0$. For large enough z_{int} we observe convergence to the analytic soliton energy of Eq. 5 (dashed lines). Larger z_{int} is required for convergence for faster solitons and/or lower densities, due to the increased soliton width. However, for the speeds and densities considered here, the integrated energy is virtually indistinguishable from the analytic prediction for $z^{\text{int}} = 4\xi$, which is employed in this work.

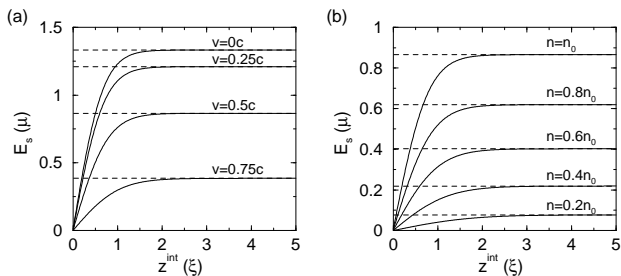


FIG. 9: Integrated local soliton energy E_s as a function of integration width z^{int} . (a) Various soliton speeds are considered in a system with peak density $n = n_0$. (b) Various values of background density n are considered for fixed soliton speed $v = 0.5c$. In each case the analytic soliton energy is indicated by a dashed line. This is performed in an infinite $V(z) = 0$ system and our units of energy and distance are the chemical potential $\mu = n_0 g$ and healing length $\xi = \hbar\sqrt{mn_0g}$ of the $n = n_0$ system.

-
- [1] D. Krökel, N. J. Halas, G. Giuliani and D. Grischkowsky, Phys. Rev. Lett. **60**, 29 (1988); G. A. Swartzlander, D. R. Andersen, J. J. Regan, H. Yin and A. E. Kaplan, Phys. Rev. Lett. **66**, 1583 (1991).
 - [2] B. Denardo, W. Wright, S. Putterman and A. Larraza, Phys. Rev. Lett. **64**, 1518 (1990).
 - [3] M. Chen, M. A. Tsankov, J. M. Nash and C. E. Patton, Phys. Rev. Lett. **70**, 1707 (1993).
 - [4] S. Burger *et al.*, Phys. Rev. Lett. **83**, 5198 (1999).
 - [5] J. Denschlag *et al.*, Science **287**, 97 (2000).
 - [6] B. P. Anderson *et al.*, Phys. Rev. Lett. **86**, 2926 (2001).
 - [7] Z. Dutton, M. Budde, C. Slowe, and L. V. Hau, Science **293**, 663 (2001).
 - [8] A. Weller *et al.*, Phys. Rev. Lett. **101**, 130401 (2008).
 - [9] C. Becker *et al.*, Nat. Phys. **4**, 496 (2008).
 - [10] S. Stellmer *et al.*, Phys. Rev. Lett. **101**, 120406 (2008).
 - [11] P. G. Kevrekidis, D. J. Frantzeskakis and R. Carretero-Gonzalez (Eds.), *Emergent Nonlinear Phenomena in Bose-Einstein condensates* (Springer, Berlin, 2008).
 - [12] P.O. Fedichev, A.E. Muryshev, and G.V. Shlyapnikov, Phys. Rev. A **60**, 3220 (1999).
 - [13] A. E. Muryshev, G. V. Shlyapnikov, W. Ertmer, K. Sen-gstock and M. Lewenstein, Phys. Rev. Lett. **89**, 110401 (2002).
 - [14] B. Jackson, C. F. Barenghi and N. P. Proukakis, J. Low Temp. Phys. **148**, 387 (2007).
 - [15] B. Jackson, N. P. Proukakis and C. F. Barenghi, Phys. Rev. A **75**, 051601(R) (2007).
 - [16] A.E. Muryshev, H.B. van Linden van den Heuvell, and G.V. Shlyapnikov, Phys. Rev. A **60**, R2665 (1999).
 - [17] L. D. Carr, M. A. Leung and W. P. Reinhardt, J. Phys. B **33**, 3983 (2000).
 - [18] D.L. Feder, M. S. Pindzola, L. A. Collins, B. I. Schneider and C. W. Clark, Phys. Rev. A **62**, 053606 (2000).
 - [19] J. Brand and W.P. Reinhardt, Phys. Rev. A **65**, 043612 (2002).
 - [20] N.P. Proukakis *et al.*, J. Opt. B **6**, S380 (2004).
 - [21] Under certain regimes energy-conservation reveals a periodic cycling between solitons and vortex rings, as reported in a recent experiment [22].
 - [22] I. Shomroni *et al.*, Nat. Phys. **5**, 193 (2009).
 - [23] T. Busch and J.R. Anglin, Phys. Rev. Lett. **84**, 2298 (2000).
 - [24] G. Huang, J. Szeftel, and S. Zhu, Phys. Rev. A **65**,

- 053605 (2002).
- [25] N. G. Parker, N. P. Proukakis, M. Leadbeater, and C. S. Adams, Phys. Rev. Lett. **90**, 220401 (2003).
 - [26] D. E. Pelinovsky, D. J. Frantzeskakis and P. G. Kevrekidis, Phys. Rev. E **72**, 016615 (2005).
 - [27] D. E. Pelinovsky, Y. S. Kivshar, and V. V. Afanasjev, Phys. Rev. E **54**, 2015 (1996).
 - [28] N. G. Parker, N. P. Proukakis and C. S. Adams, in *Progress in Soliton Research*, edited by L. V. Chen (Nova, New York, 2005), p. 1-49.
 - [29] Y. S. Kivshar and B. Luther-Davies, Phys. Rep. **298**, 81 (1998).
 - [30] N. G. Parker, N. P. Proukakis, M. Leadbeater, and C. S. Adams, J. Phys. B **36**, 2891 (2003).
 - [31] D. Frantzeskakis *et al.*, **66**, 053608 (2002).
 - [32] V. A. Brazhnyi and V. V. Konotop, Phys. Rev. A **68**, 043613 (2003).
 - [33] N. G. Parker, N. P. Proukakis, C. F. Barenghi and C. S. Adams, Phys. Rev. Lett. **92**, 160403 (2004).
 - [34] N. P. Proukakis, N. G. Parker, C. F. Barenghi and C. S. Adams, Phys. Rev. Lett. **93**, 130408 (2004).
 - [35] A. Radouani, Phys. Rev. A **68**, 043620 (2003).
 - [36] A. Radouani, Phys. Rev. A **70**, 013602 (2004).
 - [37] N. Bilas and N. Pavloff, Phys. Rev. A **72**, 033618 (2005).
 - [38] N. G. Parker *et al.* J. Phys. B **37**, S175 (2004).
 - [39] P. G. Kevrekidis, R. Carretero-Gonzalez, G. Theocharis, D. J. Frantzeskakis, and B. A. Malomed, Phys. Rev. A **68**, 035602 (2003).
 - [40] N. Bilas and N. Pavloff, Phys. Rev. Lett. **95**, 130403 (2005).
 - [41] F. Dalfovo, S. Giorgini, L. P. Pitaevskii and S. Stringari, Rev. Mod. Phys. **71**, 463 (1999).
 - [42] N.P. Proukakis and B. Jackson, J. Phys. B **41**, 203002 (2008).
 - [43] G. Theocharis, P.G. Kevrekidis, M.K. Oberthaler and D.J. Frantzeskakis, Phys. Rev. A **76**, 045601 (2007).
 - [44] Using an appropriate initial guess, propagation of the GPE in imaginary time will converge to the ground state of the system, provided it exists [46].
 - [45] M.A. de Moura, J. Phys. A **27**, 7157 (1994); M.A. de Moura, Phys. Rev. A **37**, 4998 (1988); S.A. Morgan, R.J. Ballagh, and K. Burnett, Phys. Rev. A **55**, 4338 (1997); W.P. Reinhardt and C.W. Clark, J. Phys. B **30**, L785 (1997).
 - [46] A. Minguzzi, S. Succi, F. Toschi, M. P. Tosi and P. Vignolo, Phys. Rep. **395**, 223 (2004).
 - [47] V. Bretin, S. Stock, Y. Seurin and J. Dalibard, Phys. Rev. Lett. **92**, 050403 (2004).
 - [48] W. F. Vinen, Phys. Rev. B **61**, 1410 (2000); W. F. Vinen, Phys. Rev. B **64**, 134520 (2001).
 - [49] E. Lundh and P. Ao, Phys. Rev. A **61**, 063612 (2000).
 - [50] L. M. Pismen, *Vortices in nonlinear fields* (Clarendon Press, Oxford, 1999).
 - [51] C. F. Barenghi, N. G. Parker, N. P. Proukakis and C. S. Adams, J. Low Temp. Phys. **138**, 629 (2005)
 - [52] N. S. Ginsberg, J. Brand and L. V. Hau, Phys. Rev. Lett. **94**, 040403 (2005).